

Micro- and nanoelectronics. Condensed matter physics
Микро- и нанoeлектроника. Физика конденсированного состояния

UDC 538.915

<https://doi.org/10.32362/2500-316X-2022-10-3-56-63>

RESEARCH ARTICLE

Modeling of two-dimensional $\text{Mo}_x\text{W}_{1-x}\text{S}_{2y}\text{Se}_{2(1-y)}$ alloy band structure

Nikita Yu. Pimenov[@],
Sergey D. Lavrov,
Andrey V. Kudryavtsev,
Artur Yu. Avdizhiyan

MIREA – Russian Technological University, Moscow, 119454 Russia

[@] Corresponding author, e-mail: nikitapimenov13@gmail.com

Abstract

Objectives. Two-dimensional transition metal dichalcogenides (TMDs) are utilized for various optical applications due to the presence in these materials of a direct band gap corresponding to the visible and near-infrared spectral regions. However, a limited set of existing TMDs makes the region of the used spectral range discrete. The most effective way to solve this problem is to use two-dimensional TMD films based on multicomponent alloys, including three or more different chemical elements (while TMDs consist of two). By varying their morphological composition, one can control the value of the band gap and thus their optical absorption spectrum. However, since the band gap in such structures is highly nonlinear as far as their chemical composition is concerned, it can be challenging to select the required concentration in order to achieve uniform absorption. In this regard, the purpose of this work is to theoretically determine the dependence of the band gap of four-component two-dimensional $\text{Mo}_x\text{W}_{1-x}\text{S}_{2y}\text{Se}_{2(1-y)}$ alloys on their morphological composition.

Methods. The calculations were performed within the framework of the density functional theory using the Quantum Espresso software package. Flakes of two-dimensional TMDs alloys were prepared from bulk TMDs crystals by mechanical exfoliation on a Si/SiO₂ substrate. An experimental study of the photoluminescence characteristics was carried out using photoluminescence microscopy-spectroscopy.

Results. In this work, the dependence of the band gap on the morphological composition of two-dimensional $\text{Mo}_x\text{W}_{1-x}\text{S}_{2y}\text{Se}_{2(1-y)}$ alloys was determined. Upon varying the composition of TMDs alloys, it was found that the band gap changes from 1.43 to 1.83 eV. The obtained theoretical results are in qualitative agreement with the experimental data.

Conclusions. The minimum band gap is observed in alloys close to MoSe₂, while alloys close to WS₂ have the maximum band gap value.

Keywords: transition metal dichalcogenides, two-dimensional semiconductors, band structure, band gap, density functional theory

• Submitted: 17.11.2021 • Revised: 24.02.2022 • Accepted: 19.04.2022

For citation: Pimenov N.Yu., Lavrov S.D., Kudryavtsev A.V., Avdizhiyan A.Yu. Modeling of two-dimensional $\text{Mo}_x\text{W}_{1-x}\text{S}_{2y}\text{Se}_{2(1-y)}$ alloy band structure. *Russ. Technol. J.* 2022;10(3):56–63. <https://doi.org/10.32362/2500-316X-2022-10-3-56-63>

Financial disclosure: The authors have no a financial or property interest in any material or method mentioned.

The authors declare no conflicts of interest.

НАУЧНАЯ СТАТЬЯ

Моделирование зонной структуры двумерных твердых растворов $\text{Mo}_x\text{W}_{1-x}\text{S}_{2y}\text{Se}_{2(1-y)}$

Н.Ю. Пименов[@],
С.Д. Лавров,
А.В. Кудрявцев,
А.Ю. Авдизиян

МИРЭА – Российский технологический университет, Москва, 119454 Россия

[@] Автор для переписки, e-mail: nikitapimenov13@gmail.com

Резюме

Цели. Благодаря наличию прямозонного перехода с шириной запрещенной зоны, соответствующей видимой и ближней инфракрасной областям спектра, двумерные дихалькогениды переходных металлов (ДПМ) находят применение в различных оптических приложениях. Однако ограниченный набор существующих ДПМ делает область используемого спектрального диапазона дискретной. Наиболее эффективным способом решения этой проблемы является использование двумерных пленок ДПМ на основе многокомпонентных твердых растворов, в состав которых входят три и более различных химических элемента (в то время, как ДПМ состоят из двух). Варьируя их морфологический состав, можно управлять значением ширины запрещенной зоны, и, таким образом, их оптическим спектром поглощения. Так как ширина запрещенной зоны в таких структурах сильно нелинейна по отношению к их химическому составу, это затрудняет подбор необходимой концентрации для достижения равномерного поглощения. В связи с этим целью данной работы является теоретическое определение зависимости ширины запрещенной зоны четырехкомпонентных двумерных твердых растворов $\text{Mo}_x\text{W}_{1-x}\text{S}_{2y}\text{Se}_{2(1-y)}$ от их морфологического состава.

Методы. Расчеты выполнены в рамках теории функционала плотности с использованием программного пакета *Quantum Espresso*. Двумерные кристаллиты твердых растворов ДПМ были изготовлены из объемных кристаллов ДПМ методикой механической эксфолиации на подложку Si/SiO₂. Экспериментальное исследование фотoluminesцентных характеристик было проведено при помощи фотoluminesцентной микроскопии-спектроскопии.

Результаты. В работе была определена зависимость ширины запрещенной зоны от морфологического состава двумерных твердых растворов $\text{Mo}_x\text{W}_{1-x}\text{S}_{2y}\text{Se}_{2(1-y)}$. Установлено, что при варьировании состава твердых растворов ДПМ ширина запрещенной зоны изменяется от 1.43 до 1.83 эВ. Показано, что полученные теоретические результаты качественно совпадают с экспериментальными данными.

Выводы. Минимальной шириной запрещенной зоны обладают твердые растворы, близкие по своему составу к MoSe₂, в то время как максимальной – структуры, близкие по своему составу к WS₂.

Ключевые слова: дихалькогениды переходных металлов, двумерные полупроводники, зонная структура, запрещенная зона, теория функционала плотности

• Поступила: 17.11.2021 • Доработана: 24.02.2022 • Принята к опубликованию: 19.04.2022

Для цитирования: Пименов Н.Ю., Лавров С.Д., Кудрявцев А.В., Авдигиян А.Ю. Моделирование зонной структуры двумерных твердых растворов $\text{Mo}_x\text{W}_{1-x}\text{S}_{2y}\text{Se}_{2(1-y)}$. *Russ. Technol. J.* 2022;10(3):56–63. <https://doi.org/10.32362/2500-316X-2022-10-3-56-63>

Прозрачность финансовой деятельности: Авторы не имеют финансовой заинтересованности в представленных материалах или методах.

Авторы заявляют об отсутствии конфликта интересов.

INTRODUCTION

The discovery by Novoselov and Geim of a method for obtaining graphene in 2004 [1] aroused great interest in the study of various two-dimensional materials demonstrating unique physical properties. Transition metal dichalcogenides (TMDs) can be distinguished among such materials. TMDs comprise materials having the formula MX_2 , where M is a transition metal (Mo, W, etc.) while X is a chalcogen (S, Se, etc.). The metal and chalcogen atoms have a predominantly covalent bond forming a hexagonal lattice. Bulk crystals have a layered structure with weak Van der Waals interactions between layers [2]. Unlike graphene, which has the characteristics of a semimetal, two-dimensional TMDs have a band gap. The key feature of such materials is a strong change in the configuration of their band structure with a change in thickness: for example, bulk TMD crystals are indirect-gap semiconductors, while two-dimensional crystals are referred to as direct-gap semiconductors [3]. Due to their direct transition-, high charge carrier mobility-, and a number of other properties [4], two-dimensional TMDs can be used as materials for creating photodetectors [5], phototransistors [6], solar cells [7], and other opto- and nanoelectronic devices [8].

The parameters of devices made on the basis of TMDs can be altered by varying the number of layers, as well as their composition, deformation, etc. The direct-gap transition in two-dimensional TMDs promotes efficient absorption and generation of light, which is important in optical applications. An important characteristic that determines the optical absorption of a material is the band gap. In two-dimensional TMDs, the band gap is on the order of 1–2 eV, which corresponds to the visible and near infrared regions of the spectrum. Since the number of available TMDs is very limited, the region of the spectral range used is discrete. One approach to solving this problem, which involves the synthesis of various structures comprising more than two types of atoms is possible due to the similar atomic structure of various TMDs, allowing the creation of alloys based on them (for example, $\text{MoS}_{2x}\text{Se}_{2(1-x)}$ or $\text{Mo}_x\text{W}_{x-1}\text{S}_2$) [9]. In addition, many works have been devoted to the

creation and study of heterostructures consisting of two TPM layers of different composition (for example, MoS_2/WS_2) [10] and “Janus monolayers” (materials having the formula MXY , where M is a transition metal atom enclosed between two homogeneous layers of different chalcogens X and Y), such as MoSSe or WSSe [11].

The use of alloys of two-dimensional TMDs is due to the fact that, by changing the morphological composition, one can quite accurately control the band gap. This, in turn, allows for controlling the absorption spectrum over the entire range of possible values. The non-linear nature of the dependence of the band gap on the morphological composition of the solid solution makes it difficult to select the required concentration to achieve the required parameters. In this regard, there is a need to determine this dependence.

At present, although there is a large number of works devoted to the study of three-component structures [12, 13], more complex structures remain poorly studied. In this regard, within the framework of the present work, a theoretical calculation of the band structure of two-dimensional $\text{Mo}_x\text{W}_{1-x}\text{S}_{2y}\text{Se}_{2(1-y)}$ alloys at $x, y \in 0-1$ was carried out to determine the dependence of the band gap on the morphological composition.

METHODS

All calculations in this work were carried out from first principles (*ab initio*) within the framework of density functional theory (DFT) involving the Perdew–Burke–Eisenhöff exchange-correlation functional [14] and ultrasoft pseudopotentials. The calculations were performed in the Quantum Espresso software environment [15]. The minimum cutoff kinetic energy was selected as 80 Ry, while the dimensions of the k -point sampling grid were $8 \times 8 \times 1$. The generation of singular k -points in the first Brillouin zone was performed by the Monkhrust–Pack method [16]. The unit cell of a monolayer TMD contains 1 metal atom and 2 chalcogen atoms. For calculations, a supercell was generated with a dimension of 2×2 unit cells and including 4 metal atoms and 8 chalcogen atoms. The supercell structure is shown in Fig. 1.

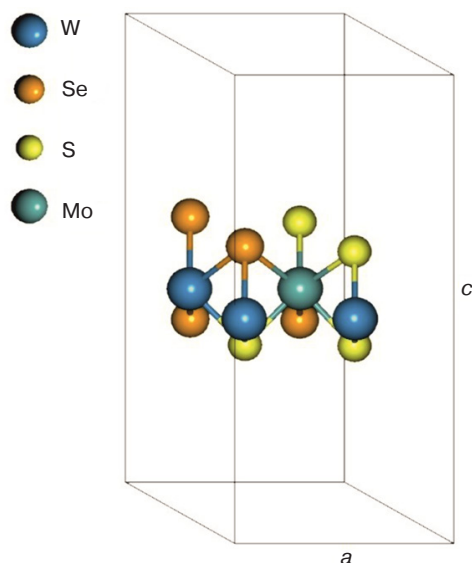


Fig. 1. Structure of the $2 \times 2 \text{ Mo}_x\text{W}_{1-x}\text{S}_{2y}\text{Se}_{2(1-y)}$ supercell

In order to eliminate the influence of neighboring layers, the cell parameter ratio c/a was set to about 2.5.

Two-dimensional TMD alloy crystallites were fabricated from commercially available bulk TMD crystals (6Carbon Technology, Shenzhen, China)¹ by mechanical exfoliation onto a Si/SiO₂ substrate. The initial samples were a series of $\text{MoS}_{2x}\text{Se}_{2(x-1)}$ with different chalcogen concentrations. The parameter x in the series varied from 0 to 1 with a step of 0.1–0.2. The presence of interference effects allowed the thickness of the created two-dimensional crystallites to be estimated using optical confocal microscopy [17].

An experimental study of the photoluminescent characteristics of the created two-dimensional solid solutions of semiconductors was carried out using photoluminescent microscopy-spectroscopy. A solid-state laser having a wavelength of 532 nm was used as a laser pump source. Next, the radiation was focused by an objective on the sample fixed on the scanning stage. The power density of the optical pump radiation was approximately 15 mW/μm². A photomultiplier coupled to an optical monochromator was used for detecting optical radiation.

RESULTS AND DISCUSSION

The band structures of two-dimensional $\text{Mo}_x\text{W}_{1-x}\text{S}_{2y}\text{Se}_{2(1-y)}$ alloys were calculated in several stages. First, the two-component TMDs— MoS_2 , WS_2 , MoSe_2 , and WSe_2 —were calculated using the corresponding unit cells. After that, the obtained results were compared with the calculations carried

out earlier using a similar method. At the second stage, three-component TMDs $\text{Mo}_x\text{W}_{1-x}\text{S}_2$, $\text{Mo}_x\text{W}_{1-x}\text{Se}_2$, $\text{MoS}_{2y}\text{Se}_{2(1-y)}$, and $\text{WS}_{2y}\text{Se}_{2(1-y)}$ of various morphological compositions were calculated. At the final stage, the four-component TMDs $\text{Mo}_x\text{W}_{1-x}\text{S}_{2y}\text{Se}_{2(1-y)}$ were calculated and a general graph of the dependence of the band gap on the morphological composition of the structures under study was constructed.

The band structures of two-dimensional MoS_2 , MoSe_2 , WS_2 , and WSe_2 calculated at the first stage are shown in Fig. 2.

In all calculated structures, a direct-gap transition is observed at the K point of the Brillouin zone. The band gap E_g , the unit cell parameter a obtained in the course of calculations, and the results obtained using a similar technique [18] are shown in Table.

Table. Theoretical results for two-component TMDs

TMD	$a_{\text{theor}}, \text{\AA}$	$a, \text{\AA}$ [18]	$E_{g \text{ theor}}, \text{eV}$	E_g, eV [18]
MoS_2	3.18	3.18	1.69	1.68
MoSe_2	3.32	3.32	1.44	1.45
WS_2	3.19	3.18	1.79	1.82
WSe_2	3.33	3.32	1.55	1.55

The calculation of three-component TMD alloys was carried out for two cases, the first when the concentration of transition metal atoms changes and the second at an altered concentration of chalcogen atoms. Figure 3 shows the dependences of the band gap E_g and the supercell parameter a for two-dimensional $\text{Mo}_x\text{W}_{1-x}\text{S}_2$ and $\text{Mo}_x\text{W}_{1-x}\text{Se}_2$ alloys on changes in the concentration of transition metals in their composition.

Both cases are characterised by a decrease in the band gap with the predominance of Mo. The $\text{Mo}_x\text{W}_{1-x}\text{S}_2$ alloys are also characterized by a larger band gap than $\text{Mo}_x\text{W}_{1-x}\text{Se}_2$ by 0.3 eV on average. The supercell parameter varies insignificantly (within a few hundredths of Å) and is on average 6.36 Å and 6.64 Å for $\text{Mo}_x\text{W}_{1-x}\text{S}_2$ and $\text{Mo}_x\text{W}_{1-x}\text{Se}_2$, respectively.

Similar calculation results for the dependences $\text{MoS}_{2y}\text{Se}_{2(1-y)}$ and $\text{WS}_{2y}\text{Se}_{2(1-y)}$ having different chalcogen ratios are shown in Fig. 4.

For both alloys, an increase in the concentration of S in the composition leads to an increased the band gap; in this case, the supercell parameter decreases with the predominance of S in the composition (by about 0.3 Å when going from Se to S).

To experimentally verify the theoretical results, the luminescence spectra of two-dimensional TMD alloys created by mechanical exfoliation were obtained. The obtained luminescence spectra are shown in Fig. 5a. It can be seen that all spectra have a characteristic

¹ URL: <http://www.6carbon.com/index-en.php>. Accessed August 3, 2021.

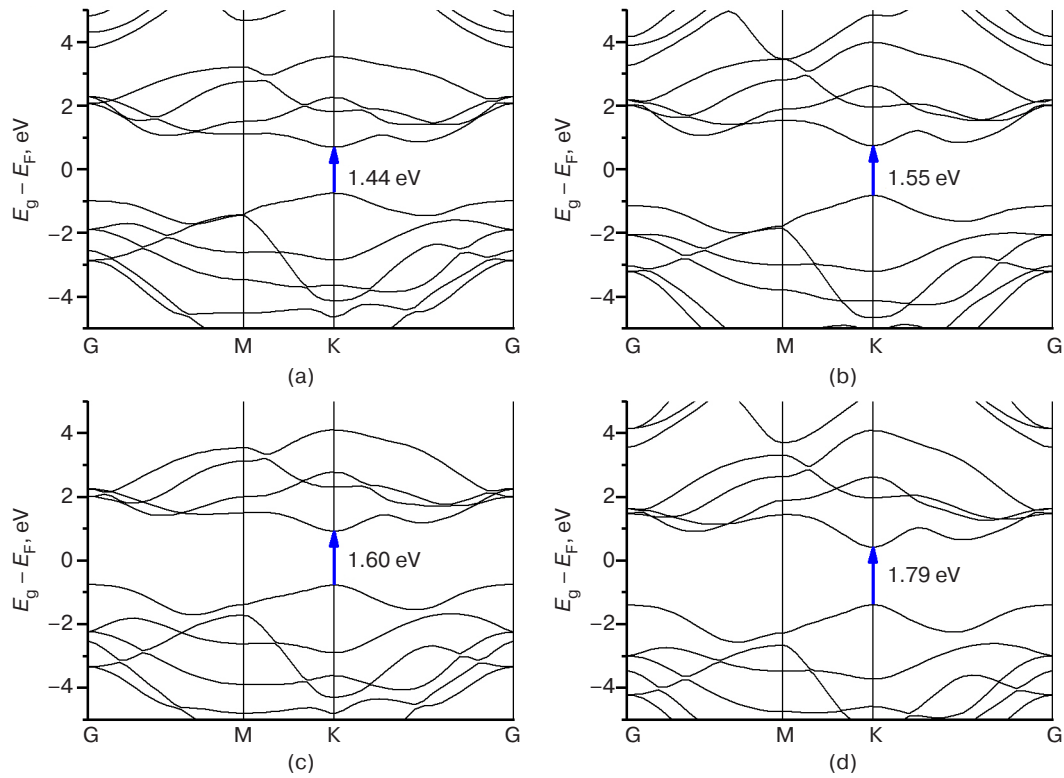


Fig. 2. Calculated band structures of (a) MoSe_2 , (b) WSe_2 , (c) MoS_2 , and (d) WSe_2 . G, K, and M are the characteristic points of the Brillouin zone

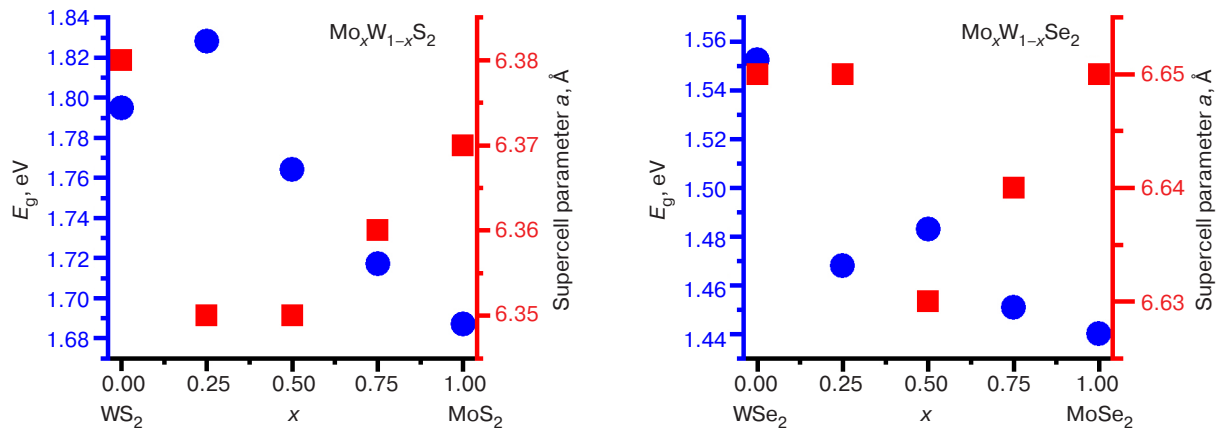


Fig. 3. Dependence of the band gap (circle) and the supercell parameter (square) on the ratio of transition metals for $\text{Mo}_x\text{W}_{1-x}\text{S}_2$ and $\text{Mo}_x\text{W}_{1-x}\text{Se}_2$, where x is the relative concentration of Mo atoms in the composition

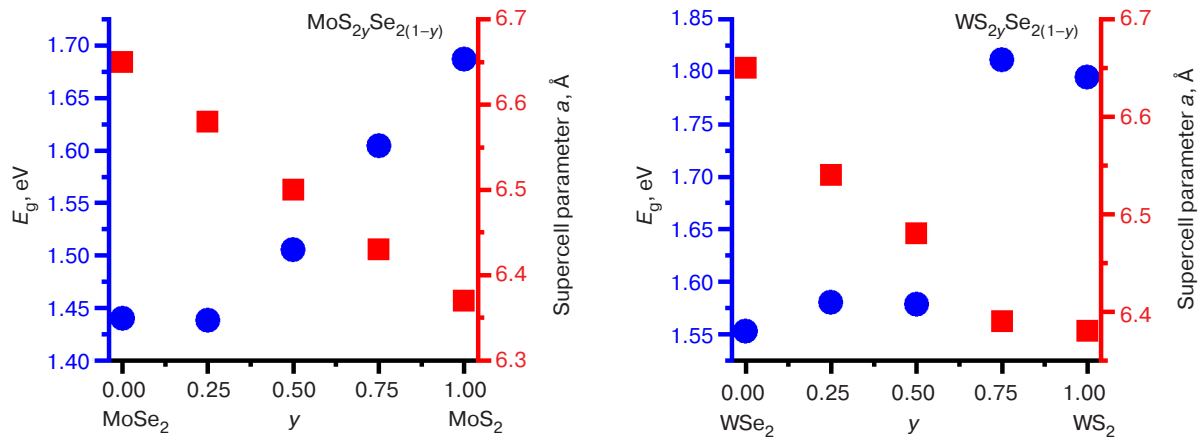


Fig. 4. Dependence of the band gap (circle) and the supercell parameter (square) on the ratio of chalcogens for $\text{MoS}_{2y}\text{Se}_{2(1-y)}$ and $\text{WS}_{2y}\text{Se}_{2(1-y)}$, where y is the relative concentration of S atoms in the composition

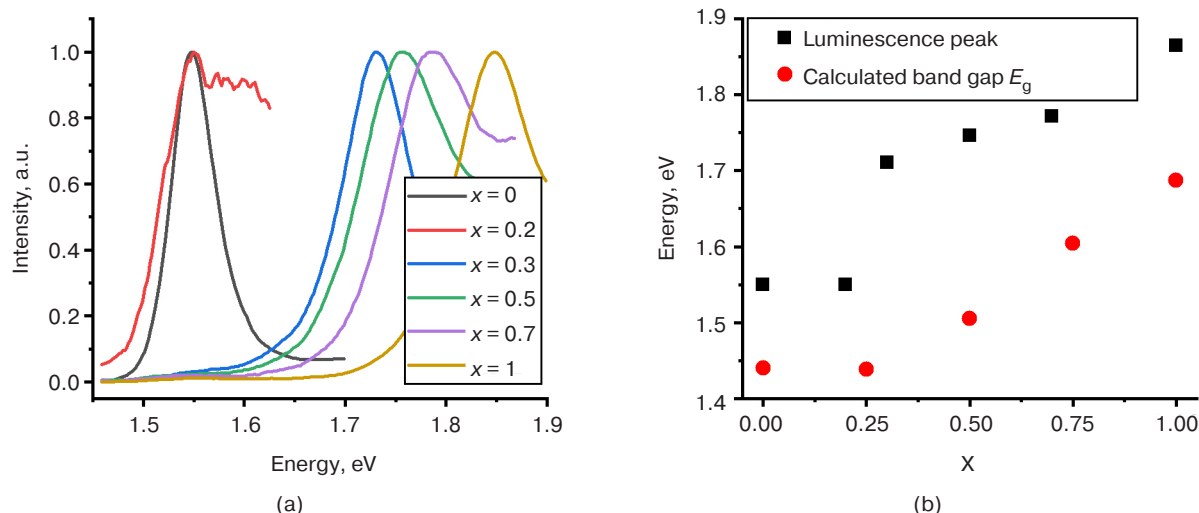


Fig. 5. (a) Luminescence spectra of alloys of two-dimensional TPM crystallites of $\text{MoS}_{2x}\text{Se}_{2(x-1)}$; (b) comparison of the theoretically calculated band gap of $\text{MoS}_{2x}\text{Se}_{2(x-1)}$ and the position of the maximum of their luminescence peak. X is the x value for $\text{MoS}_{2x}\text{Se}_{2(x-1)}$

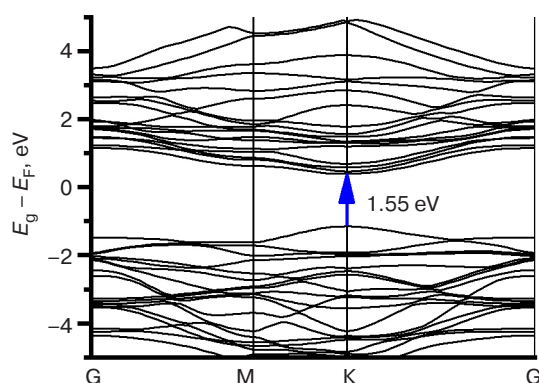


Fig. 6. Calculated band structure of the $\text{Mo}_{0.25}\text{W}_{0.75}\text{S}_{0.5}\text{Se}_{1.5}$ alloy

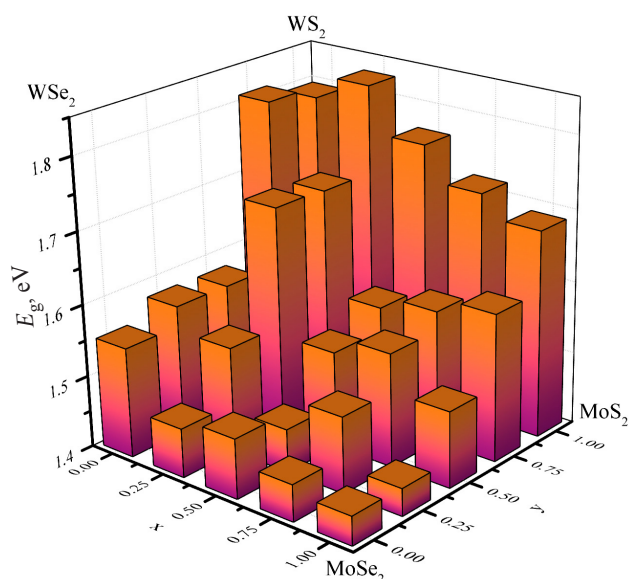


Fig. 7. Dependence of the band gap on the morphological composition of two-dimensional $\text{Mo}_x\text{W}_{1-x}\text{S}_{2y}\text{Se}_{2(1-y)}$ alloys, where x is the relative concentration of Mo atoms and y is the relative concentration of S atoms in the composition

maximum in the range from 1.55 to 1.85 eV. The positions of the maxima for each of the studied compositions are plotted together with the obtained theoretical results of the band gap in Fig. 5b. It can be seen from the presented results that the theoretical and experimental values at all TMD concentrations differ by a fixed value of approximately 0.2 eV. This is because DFT systematically underestimates the band gap; as a result, the data obtained by calculations are somewhat smaller than the experimental data [19].

The last step was the calculation of four-component $\text{Mo}_x\text{W}_{1-x}\text{S}_{2y}\text{Se}_{2(1-y)}$ alloys of various compositions. The band gap values were determined from the obtained band structures. An example of the calculated band structure for the $\text{Mo}_{0.25}\text{W}_{0.75}\text{S}_{0.5}\text{Se}_{1.5}$ alloy is shown in Fig. 6.

As in two-component alloys, a direct-gap transition is observed in all calculated four-component $\text{Mo}_x\text{W}_{1-x}\text{S}_{2y}\text{Se}_{2(1-y)}$ alloys at the K point of the Brillouin zone. Figure 7 shows the dependence of the band gap on the morphological composition of alloys of $\text{Mo}_x\text{W}_{1-x}\text{S}_{2y}\text{Se}_{2(1-y)}$ for $x, y \in 0-1$.

The results show that in two-dimensional $\text{Mo}_x\text{W}_{1-x}\text{S}_{2y}\text{Se}_{2(1-y)}$ alloys of various morphological compositions, the band gap can be varied within the range of 1.83 eV to 1.43 eV. In this case, the minimum values of the band gap have similar morphological composition structures to the MoSe_2 monolayer, while the maximum values are similar to those of the WS_2 monolayer.

CONCLUSIONS

In this work, a theoretical calculation of the band structure of monolayer $\text{Mo}_x\text{W}_{1-x}\text{S}_{2y}\text{Se}_{2(1-y)}$ alloys was carried out. It was determined that all the calculated structures are direct-gap semiconductors with a transition to the K point of the Brillouin zone. It is shown that the

supercell parameter depends weakly on the change in the concentration of transition metals (Mo and W) but is determined to a greater extent by the concentration of chalcogens (i.e., it decreases when going from Se to S). In two-dimensional $\text{Mo}_x\text{W}_{1-x}\text{S}_2\text{ySe}_{2(1-y)}$ alloys, it is possible to obtain structures having a band gap ranging from 1.43 eV (for alloys with the compositions close to that of MoSe_2) to 1.83 eV (for alloys with the compositions close to WS_2). A comparison of the theoretical results with the experimental data showed a qualitative agreement of the dependences. In this case, it is important to take into account that DFT systematically underestimates the band gap by approximately 0.2 eV. Further improvement of the obtained results implies an increase in the dimension of the supercell, making

it possible to obtain band gap values for a larger set of $\text{Mo}_x\text{W}_{1-x}\text{S}_2\text{ySe}_{2(1-y)}$ structures of various morphological compositions.

ACKNOWLEDGMENTS

This work was supported by the Russian Science Foundation (grant No. 19-72-10165). Experimental studies were carried out using the equipment of the Center for Collective Use at the MIREA – Russian Technological University.

Authors' contributions

N.Yu. Pimenov and **A.V. Kudryavtsev**—zone structure simulation of the alloys under study.

S.D. Lavrov and **A.Yu. Avdizhiyan**—experimental study of photoluminescent characteristics of alloys.

REFERENCES

1. Novoselov K.S., Geim A.K., Morozov S.V., Jiang D., Zhang Y., Dubonos S.V., Grigorieva I.V., Firsov A.A. Electric field effect in atomically thin carbon films. *Science*. 2004;306(5696):666–669. <https://doi.org/10.1126/science.1102896>
2. Chernozatonskii L.A., Artyukh A.A. Quasi-two-dimensional transition metal dichalcogenides: structure, synthesis, properties, and applications. *Phys.-Usp.* 2018;61(1):2–28. <https://doi.org/10.3367/UFNe.2017.02.038065>
3. Yun W.S., Han S.W., Hong S.C., Kim I.G., Lee J.D. Thickness and strain effects on electronic structures of transition metal dichalcogenides: 2H-MX₂ semiconductors (M = Mo, W; X = S, Se, Te). *Phys. Rev. B*. 2012;85(3):033305. <https://doi.org/10.1103/PhysRevB.85.033305>
4. Huo N., Yang Y., Wu Y.-N., Zhang X.-G., Pantelides S.T., Konstantatos G. High carrier mobility in monolayer CVD-grown MoS_2 through phonon suppression. *Nanoscale*. 2018;10(31):15071–15077. <https://doi.org/10.1039/C8NR04416C>
5. Taffelli A., Diré S., Quaranta A., Pancheri L. MoS_2 Based photodetectors: a review. *Sensors*. 2021;21(8):2758. <https://doi.org/10.3390/s21082758>
6. Shin G. H., Park C., Lee H.J., Jin H.J., Choi S.-Y. Ultrasensitive phototransistor based on WSe_2 - MoS_2 van der Waals heterojunction. *Nano Lett.* 2020;20(8):5741–5748. <https://doi.org/10.1021/acs.nanolett.0c01460>
7. Wang T., Zheng F., Tang G., Cao J., You P., Zhao J., Yan F. 2D WSe_2 flakes for synergistic modulation of grain growth and charge transfer in tin-based perovskite solar cells. *Adv. Sci.* 2021;8(11):2004315. <https://doi.org/10.1002/advs.202004315>
8. Choi W., Choudhary N., Han G.H., Park J., Akinwande D., Lee Y.H. Recent development of two-dimensional transition metal dichalcogenides and their applications. *Mater. Today*. 2017;20(3):116–130. <https://doi.org/10.1016/j.mattod.2016.10.002>
9. Su S.-H., Hsu W.-T., Hsu C.-L., Chen C.-H., Chiu M.-H., Lin Y.-C., Chang W.-H., Suenaga K., He J.-H., Li L.-J. Controllable synthesis of band-gap-tunable and monolayer transition-metal dichalcogenide alloys. *Front. Energy Res.* 2014;2:27. <https://doi.org/10.3389/fenrg.2014.00027>
10. Li M.-Y., Chen C.-H., Shi Y., Li L.-J. Heterostructures based on two-dimensional layered materials and their potential applications. *Mater. Today*. 2016;19(6):322–335. <https://doi.org/10.1016/j.mattod.2015.11.003>
11. Petrić M.M., Kremser M., Barbone M., Qin Y., Sayyad Y., Shen Y., Tongay S., Finley J.J., Botello-Méndez A.R., Müller K. Raman spectrum of Janus transition metal dichalcogenide monolayers WSe_2 and MoSe_2 . *Phys. Rev. B*. 2021;103(3):035414. <https://doi.org/10.1103/PhysRevB.103.035414>
12. Ernandes C., Khalil L., Almabrouk H., Pierucci D., Zheng B., Avila J., Dudin P., Chaste J., Oehler F., Pala M., Bisti F., Brulé T., Lhuillier E., Pan A., Ouerghi A. Indirect to direct band gap crossover in two-dimensional $\text{WS}_{2(1-x)}\text{Se}_{2x}$ alloys. *npj 2D Mater. Appl.* 2021;5(1):7. <https://doi.org/10.1038/s41699-020-00187-9>
13. Wang Z., Sun J., Wang H., Lei Y., Xie Y., Wang G., Zhao Y., Li X., Xu H., Yang X., Feng L., Ma X. 2H/1T' phase $\text{WS}_{2(1-x)}\text{Te}_{2x}$ alloys grown by chemical vapor deposition with tunable band structures. *Appl. Surf. Sci.* 2020;504:144371. <https://doi.org/10.1016/j.apsusc.2019.144371>
14. Perdew J.P., Burke K., Ernzerhof M. Generalized gradient approximation made simple. *Phys. Rev. Lett.* 1996;77(18):3865–3868. <https://doi.org/10.1103/PhysRevLett.77.3865>
15. Giannozzi P., Baroni S., Bonini N., Calandra M., Car R., Cavazzoni C., Ceresoli D., Chiarotti G.L., Cococcioni M., Dabo I., Corso A.D., Gironcoli S., Fabris S., Fratesi G., Gebauer R., Gerstmann U., Gougoussis C., Kokalj A., Lazzeri M., Martin-Samos L., Marzari N., Mauri F., Mazzarello R., Paolini S., Pasquarello A., Paulatto L., Sbraccia C., Scandolo S., Sclauzero G., Seitsonen A. P., Smogunov A., Umari P., Wentzcovitch R.M. QUANTUM ESPRESSO: a modular and open-source software project for quantum simulations of materials. *J. Phys.: Condens. Matter*. 2009;21(39):395502. <https://doi.org/10.1088/0953-8984/21/39/395502>
16. Monkhorst H.J., Pack J.D. Special points for Brillouin-zone integrations. *Phys. Rev. B*. 1976;13(12):5188–5192. <https://doi.org/10.1103/PhysRevB.13.5188>

17. Li S.-L., Miyazaki H., Song H., Kuramochi H., Nakaharai S., Tsukagoshi K. Quantitative Raman spectrum and reliable thickness identification for atomic layers on insulating substrates. *ACS Nano*. 2012;6(8):7381–7388. <https://doi.org/10.1021/nn3025173>
18. Zhuang H.L., Henning R.G. Computational search for single-layer transition-metal dichalcogenide photocatalysts. *J. Phys. Chem. C*. 2013;117(40):20440–20445. <https://doi.org/10.1021/jp405808a>
19. Huang J., Wang W., Fu Q., Yang L., Zhang K., Zhang J., Xiang B. Stable electrical performance observed in large-scale monolayer $\text{WSe}_{2(1-x)}\text{S}_{2x}$ with tunable band gap. *Nanotechnology*. 2016;27(13):13LT01. <https://doi.org/10.1088/0957-4484/27/13/13LT01>

About the authors

Nikita Yu. Pimenov, Postgraduate Student, Department of Nanoelectronics, Institute for Advanced Technologies and Industrial Programming, MIREA – Russian Technological University (78, Vernadskogo pr., Moscow, 119454 Russia). E-mail: nikitapimenov13@gmail.com. ResearcherID ABB-2465-2021, <https://orcid.org/0000-0001-9882-8647>

Sergey D. Lavrov, Cand. Sci. (Phys.-Math.), Associate Professor, Senior Researcher, Department of Nanoelectronics, Institute for Advanced Technologies and Industrial Programming, MIREA – Russian Technological University (78, Vernadskogo pr., Moscow, 119454 Russia). E-mail: sdlavrov@mail.ru. Scopus Author ID 55453548100, ResearcherID G-2912-2016, <https://orcid.org/0000-0002-9432-860X>

Andrey V. Kudryavtsev, Cand. Sci. (Phys.-Math.), Associate Professor, Researcher, Department of Nanoelectronics, Institute for Advanced Technologies and Industrial Programming, MIREA – Russian Technological University (78, Vernadskogo pr., Moscow, 119454 Russia). E-mail: kudryavcev_a@mirea.ru. Scopus Author ID 55219889700, ResearcherID O-1457-2016, <https://orcid.org/0000-0002-2126-7404>

Artur Yu. Avdizhiyan, Cand. Sci. (Phys.-Math.), Junior Researcher, Department of Nanoelectronics, Institute for Advanced Technologies and Industrial Programming, MIREA – Russian Technological University (78, Vernadskogo pr., Moscow, 119454 Russia). E-mail: avdizhiyan@mirea.ru. Scopus Author ID 57200646355, ResearcherID C-2190-2018, <https://orcid.org/0000-0003-1766-5482>

Об авторах

Пименов Никита Юрьевич, аспирант кафедры нанoeлектроники Института перспективных технологий и индустриального программирования ФГБОУ ВО «МИРЭА – Российский технологический университет» (119454, Россия, Москва, пр-т Вернадского, д. 78). E-mail: nikitapimenov13@gmail.com. ResearcherID ABB-2465-2021, <https://orcid.org/0000-0001-9882-8647>

Лавров Сергей Дмитриевич, к.ф.-м.н., доцент, старший научный сотрудник кафедры нанoeлектроники Института перспективных технологий и индустриального программирования ФГБОУ ВО «МИРЭА – Российский технологический университет» (119454, Россия, Москва, пр-т Вернадского, д. 78). E-mail: sdlavrov@mail.ru. Scopus Author ID 55453548100, ResearcherID G-2912-2016, <https://orcid.org/0000-0002-9432-860X>

Кудрявцев Андрей Владимирович, к.ф.-м.н., доцент, научный сотрудник кафедры нанoeлектроники Института перспективных технологий и индустриального программирования ФГБОУ ВО «МИРЭА – Российский технологический университет» (119454, Россия, Москва, пр-т Вернадского, д. 78). E-mail: kudryavcev_a@mirea.ru. Scopus Author ID 55219889700, ResearcherID O-1457-2016, <https://orcid.org/0000-0002-2126-7404>

Авдизиян Артур Юрьевич, к.ф.-м.н., младший научный сотрудник кафедры нанoeлектроники Института перспективных технологий и индустриального программирования ФГБОУ ВО «МИРЭА – Российский технологический университет» (119454, Россия, Москва, пр-т Вернадского, д. 78). E-mail: avdizhiyan@mirea.ru. Scopus Author ID 57200646355, ResearcherID C-2190-2018, <https://orcid.org/0000-0003-1766-5482>

Translated by E. Shklovskii

Edited for English language and spelling by Thomas Beavitt